Technical University of Denmark

DTU

A new photonic crystal fiber design on the high negative ultra-flattened dispersion for both X and Y polarization modes

Mahmud, Russel Reza; Razzak, S. M Abdur; Hasan, Md Imran; Habib, Selim

Link back to DTU Orbit

DTU Library
Technical Information Center of Denmark

A New Photonic Crystal Fiber Design on the High Negative Ultra-Flattened Dispersion for Both X and Y Polarization Modes

Russel Reza Mahmud[a,b*], S.M.Abdur Razzak[a], Md. Imran Hasan[c], Md. Selim Habib[a,d]

[*] r.r.mahmud@gmail.com

[a*] *Department of Electrical and Electronic Engineering, Rajshahi University of Engineering and Technology, Rajshahi-6204, Bangladesh.*

[b] *Department of Electrical and Electronic Engineering, Ahsanullah University of Science and Technology, Dhaka-1208, Bangladesh.*

[c] *Optical Science Group, Research School of Physics and Engineering, The Australian National University, Canberra 0200 ACT, Australia.*

[d] *Department of Photonics Engineering, Technical University of Denmark, DK-2800, Kongens Lyngby, Denmark*

Abstract

Analysis of numerical design and properties of a new silica based photonic crystal fiber (PCF) are proposed in this manuscript. The design performs ulta-flattened negative chromatic dispersion (UNCD) in the optical windows 2nd and 3rd involving O to U bands in the infrared (IF) portion. The guiding properties are observed by employing a perfectly matched layer (PML) boundary in the finite-element method (FEM). The proposed design is compatible for the application of residual dispersion compensation (RDC) as it grants negative dispersion (ND) and very low scale

dispersion variation (ΔD) of $-(253.5\pm2.5)$ and $-(292\pm2)$ ps/nm/km respectively for both X and Y polarization modes within the wavelength boundary of $1.25\xleftrightarrow{\text{ to }}1.7$ μm (450-nm band). Moreover, $\pm10\%$ alteration in the optimum parameters (OP) is also studied to assess the responsiveness of the dispersion characteristics.

Keywords

Photonic Crystal Fiber; Triangular Lattice Structure; Ultra-Flattened Negative Chromatic Dispersion; Residual Dispersion Compensation.

1. Introduction

Periodic arrangement of infinitesimal channels that conduct the whole longitudinal area of the photonic crystal fibers (PCF) [1]. Properly engineering the position, dimension and number of air holes, PCFs grant some attractive properties like ultra-flattened chromatic dispersion, very high nonlinearity, lofty sloping negative dispersion, slight confinement loss (L_C), small and huge effective mode area (A_{eff}), meager bending loss and high birefringence (B) [2-4]. The property of negative flattened dispersion (being used for residual dispersion compensation), is one of the most remarkable characteristics [5-13]. However, a major drawback of the conventional single mode optical fiber (SMOF) is that during application in long transmission system, it gives positive dispersion of 12 to 22 ps/nm/km which can greatly increase when the optical signal passes over longer distance via that SMOF [2]. This positive dispersion degrades the optical pulse in all respects specially for wavelength division multiplexing (WDM). To diminish this positive dispersion, there are many techniques are used. Among them, dispersion compensation (DC) is the

most popular of all. Nevertheless, even after implementing DC, some residual dispersion still persist for few specific wavelengths which need a secondary compensation done by a fiber called residual dispersion compensation (RDC) fiber. This RDC fiber provides large negative but flatted dispersion to discard the accrued extra positive dispersion of a SMOF in an optical link. Such kind of fiber considering chromatic dispersion should be as much as high negative with flattened for reducing cost and loss.

It is mentioned worthy here that many researchers [5-13] have displayed several PCF designs with large negative but flattened dispersion property. For example, Varshney [5], Franco [7] and Tee et al. [12] proposed PCFs in conventional hexagonal pattern that confirmed very low average negative flattened dispersion (NFD) of $-(98.3\pm1.1)$, $-(179\pm2.1)$ and $-(456\pm6)$ ps/nm/km for respectively $1.48\xleftrightarrow{to}1.63$, $1.36\xleftrightarrow{to}1.69$ and $1.46\xleftrightarrow{to}1.68$ μm wavelength boundary. Owing to designed one PCF with very small diameter of air holes is placed into another single PCF, the designs of ref. 7 and 12 becoming more complex to fabricate. Again, hybrid PCFs in hexagonal [11] reported NFD with ΔD of about $-(138\pm6)$ ps/nm/km over respectively O to L wavelength bands. Furthermore, the fabrication process is difficult for the ref. 11 since the design is hybrid in structure. Besides, Silva et al. [8, 9] proposed PCFs that ensured NFD of $-(203\pm5)$ and $-(212\pm5.5)$ ps/nm/km for $1.35\xleftrightarrow{to}1.7$ μm wavelength boundary. The main challenges of [8, 9] are fabrication difficulties due to the Ge doped core structure. Moreover, out of hexagonal structure, ref. 10, 11 and 13 reported an equiangular decagonal spiral (DES) PCF. The designs of ref. 10 and 11 confirmed NFD of $-(227\pm6)$ and $-(393\pm6)$ ps/nm/km both for $1.35\xleftrightarrow{to}1.675$ μm wavelengths and ref. 13 ensured

NFD of $-(453 \pm 7)$ ps/nm/km for 1.15$\xleftarrow{\hspace{0.3em}to\hspace{0.3em}}$1.75 μm. But, the focusing problems of ref. 10, 11 and 13 are complex in design for spiral pattern i.e., it is almost impractical to fabricate such decagonal equiangular spiral PCF through the stack and draw conventional method. To the best of our literature review, a PCF with the property of UNCD can be used for DC as well as RDC. The reported PCF designs [5-10] show very low negative flattened chromatic dispersion. Besides, the mentioned residual dispersion compensation PCF designs [5-13] did not consider ultra-flattened negative chromatic dispersion (UNCD) for both X and Y polarization modes.

In this write-up, we propose numerical design and analysis of a new RDC fiber (F) having all circular air holes that are placed in a triangular pattern. The main achievements of the proposed RDCF are simple design with ultra-flattened negative chromatic dispersion (UNCD) of -251 to -256 (ΔD of ±5) ps/nm/km for X and -290 to -294 (ΔD of ±4) ps/nm/km for Y polarization mode respectively within a wide band wavelength of 1.25$\xleftarrow{\hspace{0.3em}to\hspace{0.3em}}$1.7 μm (450-nm). This bandwidth supports the optical windows 2nd and 3rd involving O+E+S+C+L+U bands in the infrared (IF) portion. The properties offering by our proposed RDCF are essential as a fiber for residual dispersion compensation (RDC) in optical communication network.

2. Geometry of the Proposed RDCF

Fig.1 views the geometry of the proposed triangular lattice structured RDC-PCF. It has air holes arrays in circular shape that are placed in a triangular position with modified central core at the light concentrating area. The potential material of the proposed RDCF is silica that has abundant advantages as host material for PCF manufacturing such as availability, favorable thermal and crystallization stability. The

surrounding cladding region has circular shape of air holes. Distance of any two-neighboring air holes either in X or Y axis in flat-out is called pitch and is equal to Λ which is the only dependable variable of parameter. All other function of parameters are numerically related and dependent on this variable. The angular displacement of
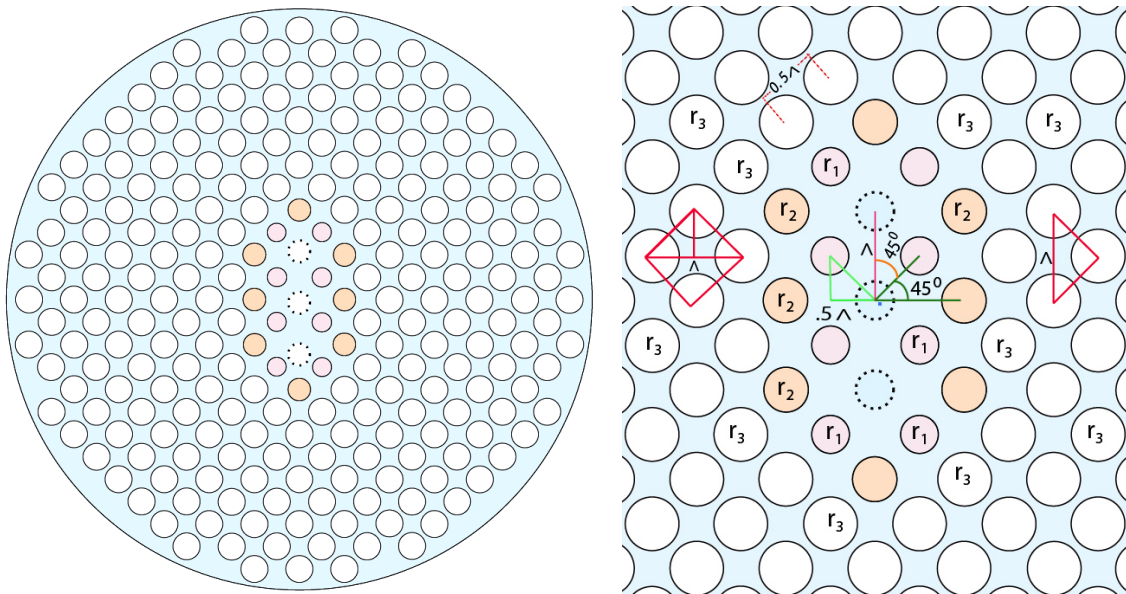

Fig.1 (a) Cross-section in the view of transversal mode of the proposed RDCF design (b) With optimized structural parameters minutely.

45^0 is created between any two nearest air holes. Therefore, any four air holes in the nearest position makes a square. Three air holes are intentionally omitted which are mentioned as dotted line in the circular shape placing core region in order to get UNCD and in Fig.1(b), it is exhibited. For optimizing and getting UNCD, we take into account the distance of pitch $\Lambda = 0.53$ μm and the diameters of the air holes array in the first and second rectangular position are $r_1 = 0.42 \times \Lambda$ and $r_2 = 0.5 \times \Lambda$. Besides r_1 and r_2, the diameter of other air holes are $r_3 = 0.6 \times \Lambda$. Fig.1 (a) displays the dotted missing circular air holes that create modification in the core portion for the raised RDCF design. Moreover, Fig.1 (b) views the design parameters for optimization minutely.

3. Equations, Results of Simulation and Discussions

Commercially available COMSOL software based on finite element method (FEM) [7, 14] is using for simulation purpose. The dispersion (D), birefringence (B), confinement loss or leakage loss (L_C) and effective area (A_{eff}) were calculated using the given equations [3, 6, 13].

$$D = -(\lambda/C)\left[\left(d^2\,\mathrm{Re}[\eta_{eff}]\right)/d\lambda^2\right] \qquad (1)$$

$$B = \left|\mathrm{Re}(\eta_{eff}^X) - \mathrm{Re}(\eta_{eff}^Y)\right| \qquad (2)$$

$$L_C = 8.686 \times k_O\,\mathrm{Im}[\eta_{eff}] \qquad (3)$$

$$A_{eff}(\lambda) = \left[\int_{-\infty}^{\infty}\int_{-\infty}^{\infty}\left(|E(x,y)|^2\right)dxdy\right]^2 / \int_{-\infty}^{\infty}\int_{-\infty}^{\infty}\left(|E(x,y)|^4\,dxdy\right) \qquad (4)$$

Dispersion (D) which is obtained as the alteration of the pulse width for the distance of propagation in per unit (i.e., ps/nm/km). In equation no.1, C= light velocity in vacuum, λ= wavelength and η_{eff}= effective refractive index. Real part of η_{eff} is need for calculating dispersion property. The wavelength dependent refractive index of optical material (silica) for the proposed RDCF is calculated using sellmeier equation for three terms. A_{eff}= The effective area measured in μm^2 is defined by putting the value of electric field into Maxwell's equation. A_{eff} is the area where the beam intensity of light drops to 13.5% of its maximum peak value. Birefringence (B) is the value defined by subtracting two effective refractive indices of X-Y polarized axes. Confinement loss represents as L_C is measured in dB/m. For getting L_C, a PML is used in FEM based comsol software. After getting the value of η_{eff} (real and imaginary part), dispersion (D), birefringence (B), confinement loss (L_C) and effective area (A_{eff}) can be evaluated by the above-mentioned equations [3, 6, 12-14].

Fig.2 views the distributions of the optical field at 1.55 µm wavelength for the fundamental X-Y polarization modes. It also shows that the beam intensity of the lights for the X and Y polarization modes are strongly confined in the central core area for the raised RDCF design since $(\eta_{eff})_{core} > (\eta_{eff})_{cladding}$.

Fig.3 shows X and Y polarized optical field distribution at 1.55 µm and the relationship between the effective refractive indices and wavelength from $1.25 \xleftrightarrow{to} 1.7$ µm with the value of optimum parameters (OP). The difference between η_{eff} of X and Y polarized modes are gained by removing two air holes in vertically up and down positions of the central core. η_{eff} of the X-Y polarized modes decreases with increasing λ. η_{eff} varies from 1.287 to 1.248 and 1.28 to 1.241 for respectively X and Y polarized modes within $1.25 \xleftrightarrow{to} 1.7$ µm wavelength. It is also observed from Fig. 3 that $(\eta_{eff})_{X\text{-Polarized}} > (\eta_{eff})_{Y\text{-Polarized}}$ since asymmetric distribution of air holes in the cladding (removing two air holes in up and down positions on the Y-axis in the central core area) and their difference provides the value of B.
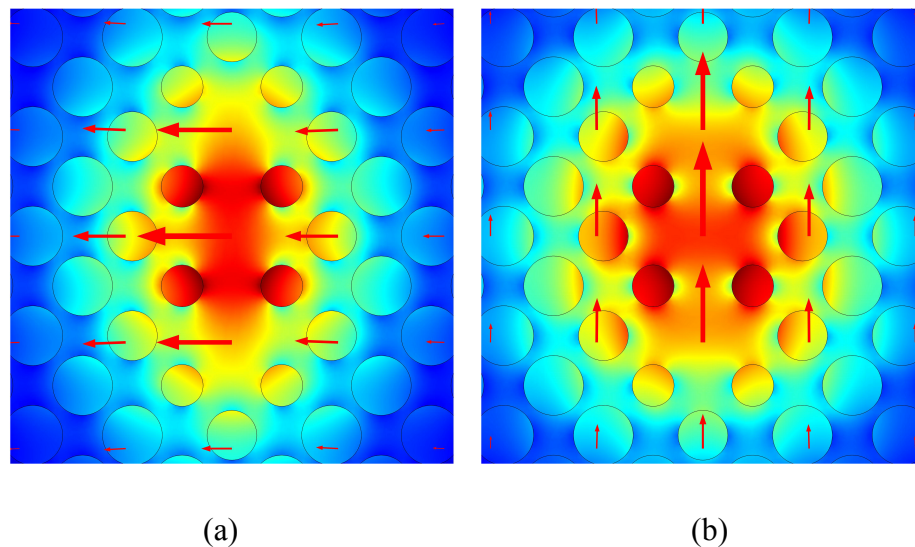

(a)   (b)

Fig.2 Optical field distribution for the fundamental modes at λ of 1.55 µm wavelength. (a) X polarized and (b) Y polarized.
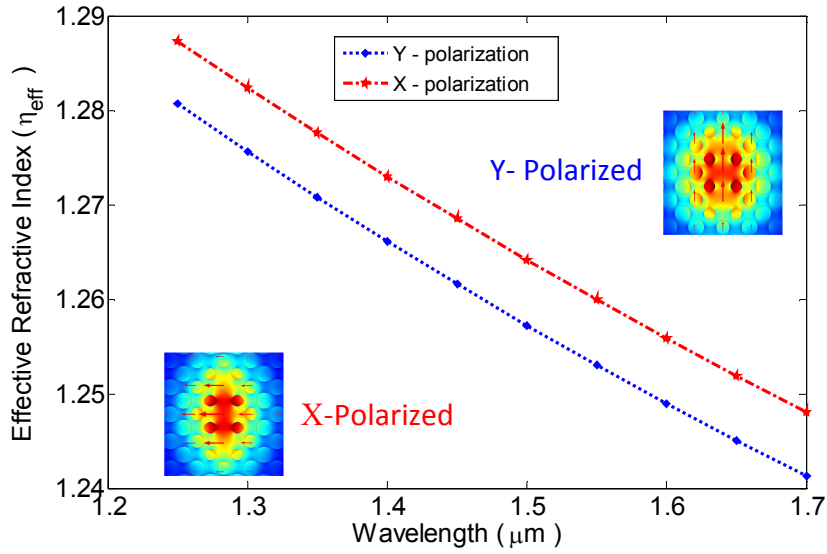
Fig.3 η_{eff} as a function of wavelength for two X-Y polarized modes with optimum parameters (OP) ($\Lambda = 0.53$ μm, $r_1 = 0.42 \times \Lambda$, $r_2 = 0.5 \times \Lambda$ and $r_3 = 0.6 \times \Lambda$) for the RDCF design.
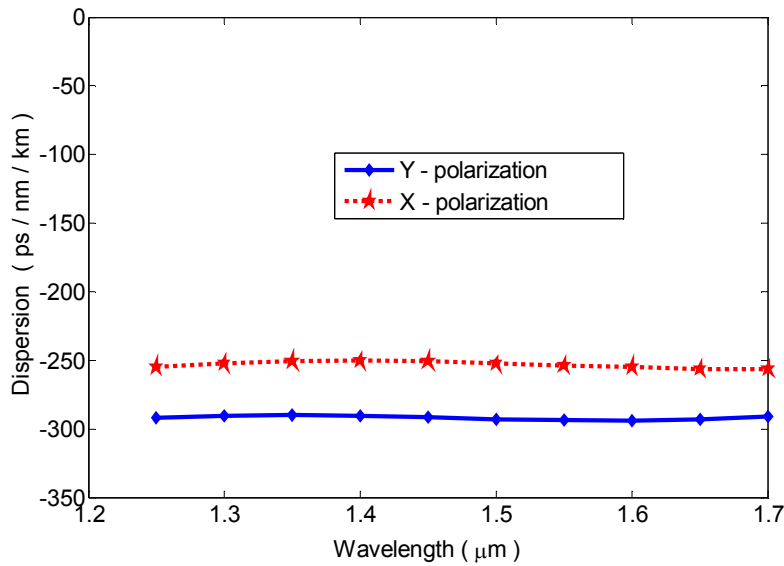

Fig.4 Responses of dispersion with wavelengths for the value of OP for Y (solid line) and X (dashed line) polarized modes for the RDCF design.

Generally, a true residual dispersion compensating fiber (RDCF) should have ultra-flattened negative chromatic dispersion (UNCD) for all wavelengths within a band for both X and Y polarized modes. In Fig.4, both Y and X polarization modes show

UNCD of $-(292 \pm 2)$ and $-(253.5 \pm 2.5)$ ps/nm/km within the wider wavelength span of $1.25 \xleftarrow{\text{to}} 1.7$ µm ($450-$nm). Chromatic dispersion can be explained by the summation of waveguide effects on dispersion and material dispersion [4]. An oscillation comes between the characteristics of dispersion depending on the value of the parameters and when the bandwidth of the particular characteristics of dispersion is significantly wide [4, 13]. Compared to other previous designs [6-13], only the proposed RDCF design performs negative ultra-flattened dispersion with the variation of only 4 and 5 ps/nm/km for the fundamental (Y and X) polarized modes. It also provides wider bandwidth than that of other PCF designs mentioned in the references [5-12]. The variables of our RDCF design are Λ, r_1, r_2 and r_3. In optimization process, one parameter is varied when other parameters are constant to see the influence on the characteristics curve for a particular property. Here for getting UNCD, the optimum parameters (OP) are chosen in such a way that the first rectangular air holes have the lower value of diameters $r_1 = 0.42 \times \Lambda$ than that of others i.e. $r_2 = 0.5 \times \Lambda$ and $r_3 = 0.6 \times \Lambda$. Here only independent variable is pitch of $\Lambda = 0.53$ µm. This design has only three variations in diameter of air holes that are helpful for fabrication.

$\pm 1\%$ alteration during fabrication creates influence on the characteristics of any PCF properties. So, it is considerable to evaluate the sensitivity of D and other properties to $\pm (1 \text{ to } 5)\%$ alteration to it's OP for ensuring dispersion fitness [16]. Keeping this in mind, numerical study has been taken for the effect of $\pm (1 \text{ to } 10)\%$ alteration in the structural parameters. The response of characteristics is done changing one parameter when all other parameters are fixed to the optimum level.
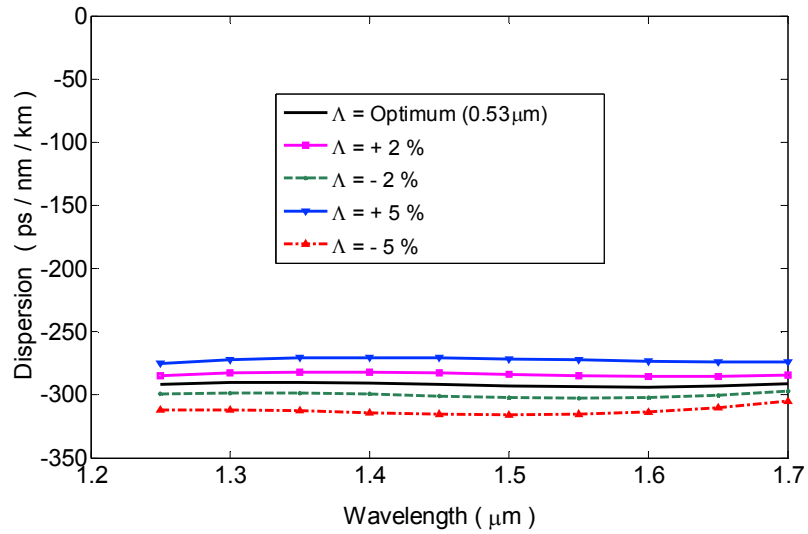
Fig.5 Responses of dispersion with wavelength for $\pm 2\%$ to $\pm 5\%$ alteration in Λ when r_1, r_2 and r_3 are kept fixed (Tokenless Solid line presents the value of OP. Additionally with token solid and dashed lines expose increment and decrement of Λ respectively)
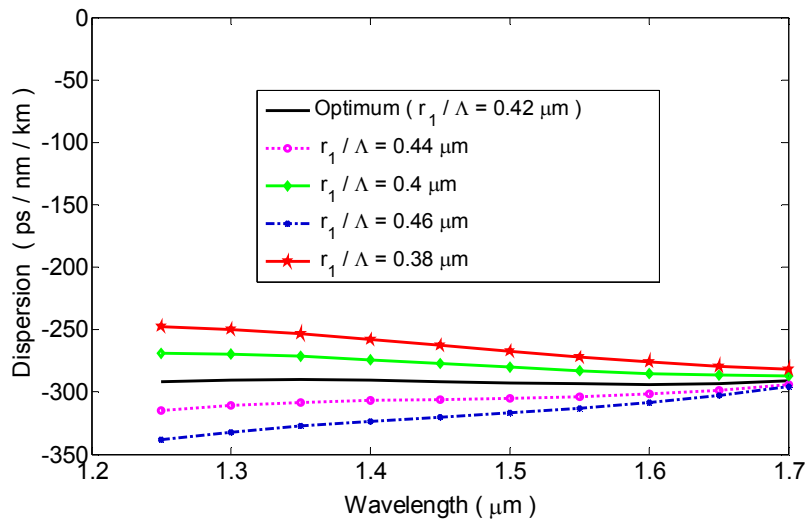

Fig.6 Responses of dispersion with wavelength for alteration r_1 (first rectangular position air holes' diameters) when Λ, r_2 and r_3 are kept constant for the RDCF. (Tokenless solid line shows value of OP. Furthermore, with token solid lines report decrement while dashed line for increment of r_1.)
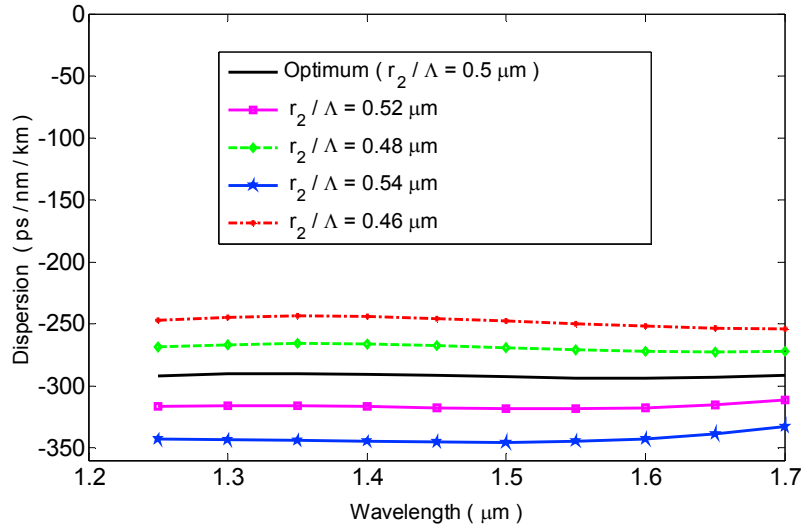
Fig.7 Responses of dispersion with wavelength by changing only r_2 (second rectangular position diameter of air holes) when other parameters Λ, r_1 and r_3 are kept constant at the value of OP. (With and without token solid lines depict value of OP and increment while dashed lines are for decrement of r_2.)
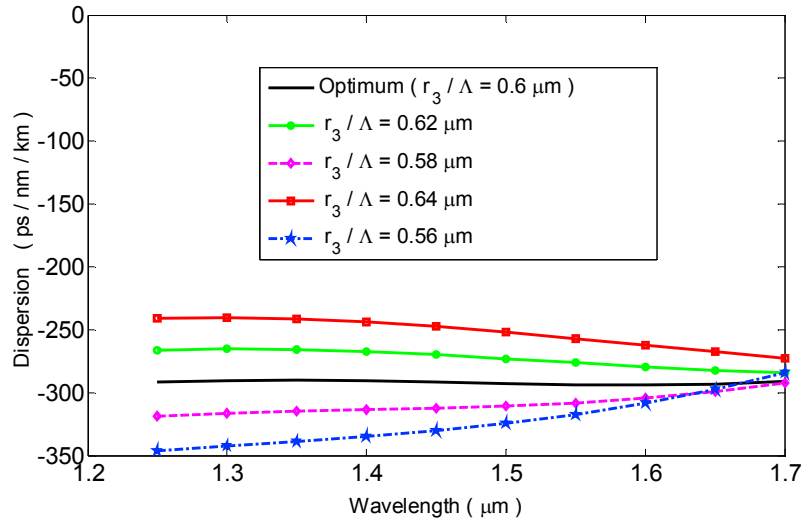

Fig.8 Responses of dispersion with wavelength for changing only r_3 when Λ, r_1 and r_2 are fixed for our proposed RDCF design. (Here solid line with token presents value of OP. On the other side, solid and dashed lines with token report increment and decrement of r_3 .)

Fig.5 views the alteration of Λ when r_1, r_2 and r_3 remain constant and from that figure it is observed that D changes ± 7 and ± 20 ps/nm/km when the alteration of Λ is carried at $\pm 2\%$ and $\pm 5\%$ respectively. So, due to the tolerance of pitch variation, *D* changes slightly. In Fig.6, the alteration of r_1 (air holes' diameter in the first rectangular position) at $\pm(0.02$ to $0.04)$ μm when all other parameters are fixed. *D* changes by only $\pm(15$ to $30)$ and $\pm(5$ to $10)$ ps/nm/km respectively from its previous optimum value for $1.25 \xleftrightarrow{to} 1.4$ and $1.5 \xleftrightarrow{to} 1.7$ μm wavelength. Moreover, air holes' diameter alteration of r_2 (second rectangular position) is given in Fig.7 when r_1, r_3 and Λ are constant. Fig.7 shows D changes ± 20 and ± 40 ps/nm/km when r_2 alternates to ± 0.02 and ± 0.04 μm. Fig.8 shows with alteration of r_3 upto ± 0.02 and ± 0.04 μm, D changes by $\pm(25$ to $50)$ and $\pm(5$ to $10)$ ps/nm/km for $1.25 \xleftrightarrow{to} 1.4$ and $1.55 \xleftrightarrow{to} 1.7$ μm wavelength respectively. Fig.9 shows alteration of all the air holes' diameter when pitch is fixed. In this study, D changes only ± 6 and ± 15 ps/nm/km when r_1, r_2 and r_3 change $\pm 2\%$ and $\pm 5\%$ together. From all observation, $\pm 5\%$ alteration of air holes' diameter report more effects than $\pm 2\%$ alteration. It is observed from Fig.10 that dispersion changes slightly and maintains the flattened characteristics with the variation of all parameters together upto $\pm(0.01$ to $0.02)$ μm from the previous value of OP. Therefore, the variations of all parameters maintain the negative flattened dispersion characteristics and that make the fabrication tolerance satisfied. From the simulation, low birefringence of 6.65×10^{-3} to 6.9×10^{-3} can be evaluated within the wide bandwidth from $1.25 \xleftrightarrow{to} 1.7$ μm with the value of OP for the RDCF design.
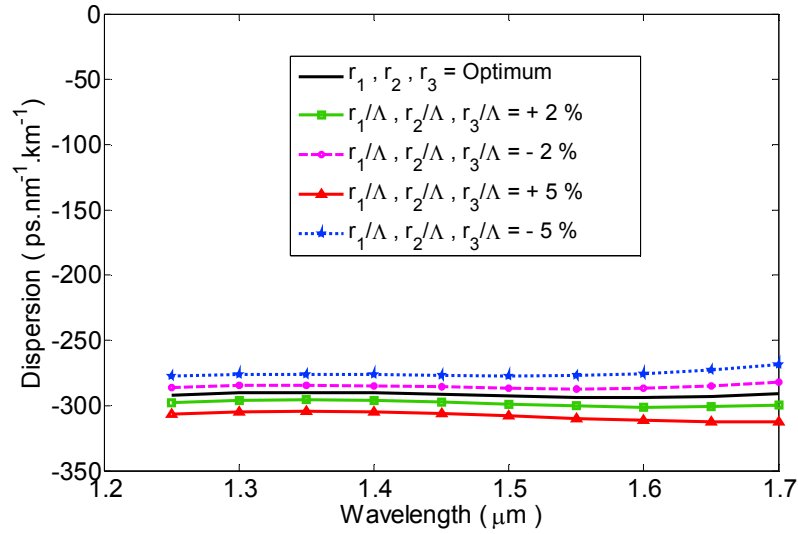
Fig.9 Responses of dispersion with wavelength for variation of only the hole air holes diameter together at $\pm 2\%$ and $\pm 5\%$ when Λ is fixed. (With token solid lines explore dispersion curve due to increment whereas dashed lines for decrement)
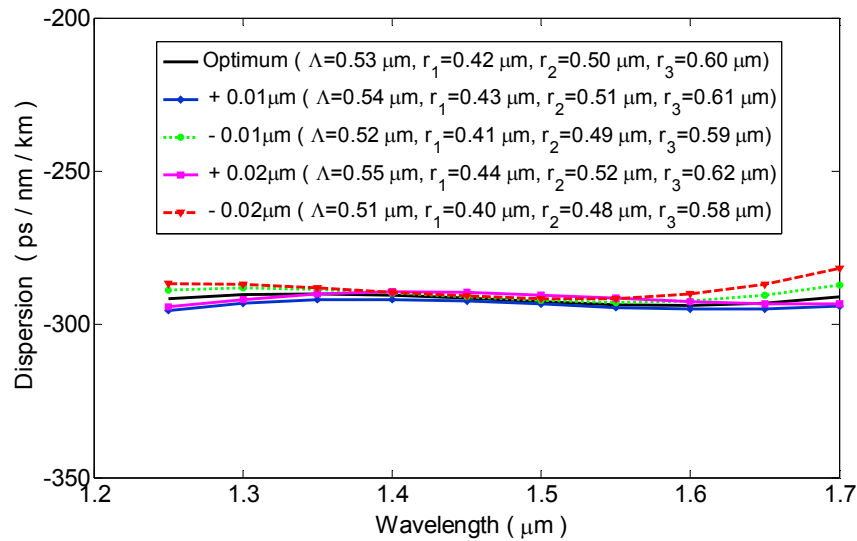

Fig.10 Responses of dispersion for altering all parameters (Λ, r_1, r_2 and r_3) together for $\pm(0.01$ to $0.02)$ µm of the raised RDCF design. (Solid line without token exposes dispersion curve and with token for increment whereas dashed lines for decrement)
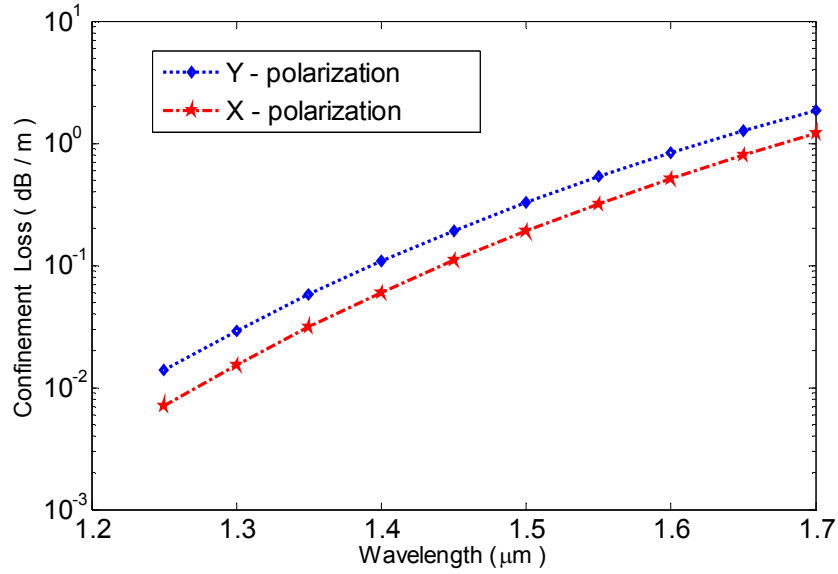
Fig.11 Responses of confinement loss with wavelength for the value of OP for both X and Y-polarization modes of the RDCF design.

Besides, we obtained effective area 1.45 to 2.05 μm^2 for Y-polarized mode and 1.13 to 1.65 μm^2 for X-polarized mode within 1.25$\xleftrightarrow{to}$1.7 μm wavelength. Splice loss will be slightly higher for the RDCF design owing to the small effective area. Nevertheless, splice loss can be reduced using fusion splicing [18]. Recently, L. Saval et al. [19] reported a splice-free interconnection technique to minimize splice loss during connecting between a SMOF and a PCF. Fig.11 shows confinement loss (L_C) at a magnitude of 10^{-2} to 10 dB/m found for X and Y polarization modes within the wavelength of 1.25$\xleftrightarrow{to}$1.7 μm. To the utmost level of our literature study, it goes without saying that confinement loss can be reduced without affecting dispersion property by adding more outer rings in the cladding area [3, 13].

During mode test, comparative study between fundamental mode and second mode considering L_C at 1.55 μm wavelength. Our proposed RDCF supports a stronger fundamental mode and in that case L_C of the second mode is higher than 46 dB/m. Moreover, L_C of the second mode higher 1246 times than the fundamental mode.

Therefore, the proposed RDCF will successfully operates as a single-mode fiber [13]. Again, for mode analysis, the effective V parameter is calculated by the equation $V_{eff} = (k_0 \Lambda F^{1/2})(n_{co}^2 - n_a^2)^{1/2}$ where n_{co} and n_a are refractive indices of core and air holes. Here F (air filling fraction) = A_{hole}/A_{cell}. Here, A_{hole} and A_{cell} are holes' and PCF's area respectively. Fig.12 reports that V_{eff} is less than 1.44402 for 1.25$\xleftrightarrow{to}$1.7 μm wavelength. So, obviously the proposed RDCF will perform like a single mode fiber.
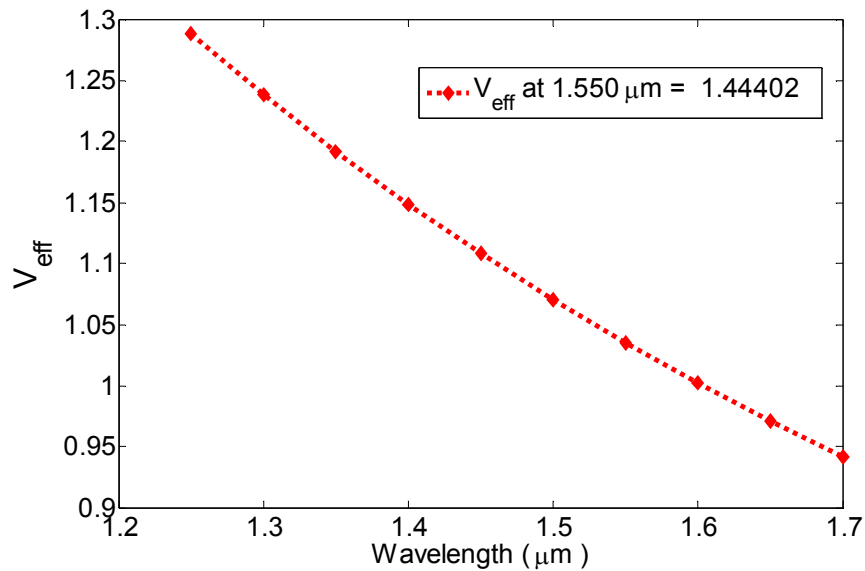
Fig.12 Response of V_{eff} parameter with wavelength for single mode test of the RDCF design.

Now only point is the fabrication issue for the proposed RDCF design. We prefer our proposed structure very similar to the common hexagonal pattern. Due to the triangular position of all the air holes of the raised design, it can be fabricated by using conventional stack and draw technique [15]. In addition, Suzuki et al. theoretically and practically examined the complex structure by adopting conventional stack and draw method [16]. Alternatively, using sol-gel method any irregular structure of PCFs can be fabricated and this method provides flexibility

during fabrication for any complex structured PCF [17]. The diameter of air hole of around 0.1 μm including fractional pitch in PCF have been fabricated using the material of silica [20]. Obviously our proposed design can be fabricated because the smallest air-hole size being 0.22 μm and the pitch being 0.53 μm (which is larger than the fabrication dimension reported in ref. 20). Moreover, using extrusion technique, air-hole size as small as 0.2 μm in the core region was already achieved in lead silicate PCF [21]. Furthermore, table 1 shows comparison between the dispersion properties for both X and Y polarization modes of the RDCF design with that of other PCFs. It is reported that only our proposed PCF provides ultra-flattened negative chromatic dispersion (UNCD) for both X and Y polarization modes whereas the other designs did not consider.

Table 1

Comparison between the properties of the proposed RDCF and those of other PCFs

PCFs	Coverage of Wavelength (μm)	Dispersion Levels for Y-polarized mode	(ΔD) ps/nm/km	Dispersion Levels for X-polarized mode	(ΔD) ps/nm/km	Covering Bands
Ref. [6]	0.98 to 1.58	--	--	-132 to -144	12	O+E+S+C
Ref. [7]	1.48 to 1.675	--	--	-178 to -180	2	S+C+L+U
Ref. [9]	1.35 to 1.7	--	--	-201 to -212	12	E+S+C+L+U
Ref. [10]	1.35 to 1.675	--	--	-391 to -399	10	E+S+C+L+U
Ref. [11]	1.35 to 1.675	--	--	-221 to -232	12	E+S+C+L+U
Ref. [12]	1.37 to 1.7	--	--	-450 to -462	12	E+S+C+L+U
Ref. [13]	1.15 to 1.7	--	--	-446 to -460	14	O+E+S+C+L+U
Proposed RDCF	1.25 to 1.7	-290 to -294	4	-251 to -256	5	O+E+S+C+L+U

Conclusion

A truly single mode ultra-flattened negative dispersion PCF has been proposed. The proposed RDCF has offered negative flattened dispersion of -251 to -256 ps/nm/km for X and -290 to -294 ps/nm/km for Y polarization modes for a wide wavelength band of $1.25 \xleftrightarrow{to} 1.7$ μm. This bandwidth covers O+E+S+C+L+U bands and supports the optical windows 2nd and 3rd in the infrared region. The proposed RDCF has circular air holes that simplify the fabrication. As a result, with the appealing features of the proposed RDCF, it is concluded that this fiber can be used as a fiber in high-speed data transmission optical network for the application of residual dispersion compensation.

References

[1]   A. Bjarklev, J. Broeng, A. S. Bjarklev, "Photonic Crystal Fibers," Kulawer Academic Press, USA, 2003.

[2]   G. P. Agrawal, Fiber Optic Communication Systems, 3rd ed. Wiley, pp. 15–64, 2002.

[3]   M.A. Hossain, Y. Namihira et al., "Polarization maintaining highly nonlinear photonic crystal fiber for supercontinuum generation at 1.55 μm," *Optics & Laser Technology*, vol. 44, no. 5, pp. 1261–1269, 2012.

[4]   P.S. Maji and P.R. Chaudhuri, "Circular Photonic Crystal Fibers: Numerical Analysis of Chromatic Dispersion and Losses," *ISRN Optics,* vol. 2013, no.2013, pp. 1-9, 2013.

[5]   S. K. Varshney, N. J. Florous, K. Saitoh, M. Koshiba, T. Fujisawa, "Numerical investigation and optimization of a photonic crystal fiber for

simultaneous dispersion compensation over S+C+L wavelengthbands," Optics Communication, vol. 274, no. 1, pp. 74-79, 2007.

[6]   M. S. Habib, M. S. Habib, M. I. Hasan, and S. M. A. Razzak, "A single mode ultra flat high negative residual dispersion compensating photonic crystal fiber," Optical Fiber Technology, vol. 20, no. 4, pp. 328-332, August 2014.

[7]   M. A. R. Franco, V. A. Serrao, and F. Sircilli, "Microstructured optical fiber for residual dispersion compensation over S+C+L+U wavelength bands," IEEE Photonics Technology Letters, vol. 20, no. 9, pp. 751-753, May 2008.

[8]   J. P. d. Silva, D. S. Bezerra, I. E. fonseca, V. F. Rodriguez-Esquerre, and H. E. Hernandez-Figueroa, "Photonic crystal fiber design with Ge-doped core for residual chromatic dispersion compensation," *in Proc. SBMO/IEEEMTT-SInt. Microw. Optoelectron. Conf. (IMOC)*, pp. 787-791, 2009.

[9]   J. P. d. Silva, D. S. Bezerra, V. F. Rodriguez-Esquerre, I. E. d. Fonseca, and H. E. Hernández-Figueroa, "Ge-doped defect-core microstructured fiber design by genetic algorithm for residual dispersion compensation," IEEE Photonics Technology Letters, vol. 22, no. 18, pp. 1337-1339, September 2010.

[10]   M. A. Islam and M. S. Alam, "Design of a polarization-maintaining equiangular spiral photonic crystal fiber for residual dispersion compensation over E+S+C+L+U wavelength bands," IEEE Photonics Technology Letters, vol. 24, no. 11, pp. 930-932, June 2012.

[11]   M. A. Islam and M. S. Alam, "Design Optimization of equiangular spiral photonic crystal fiber for large negative flat dispersion and high birefringence," IEEE Journal of Lightwave Technology, vol. 30, no. 22, pp. 3545-3551, November 2012.

[12] D. C. Tee, M. H. A. Bakar, N. Tamchek, and F. R. M. Adikan, "Photonic Crystal Fiber in Photonic Crystal Fiber for Residual Dispersion Compensation Over E+S+C+L+U Wavelength Bands," *IEEE Photonics Journal,* vol.5, no. 3, pp. 7200607, 2013.

[13] R. R. Mahmud, S. M. A. Razzak, M. I. Hasan, G. K. M. Hasanuzzaman, "Ultraflattened high negative chromatic dispersion over O+E+S+C+L+U bands of a microstructured optical fiber," *Optical Engineering,* vol. 54, no. 9, pp. 0971051-0971057, 2015.

[14] Z. Zang and Y. Zhang, "Analysis of optical switching in a Yb^{3+} -doped fiber Bragg grating by using self-phase modulation and cross-phase modulation," Applied Optics, vol. 50, no. 16, pp. 3424-3430, 2012.

[15] H. Ademgil, S. Haxha, F. A. Malek, "Highly Nonlinear Bending-Insensitive Birefringent Photonic Crystal," International Journal of Scientific & Engineering Research, vol. 2, no. 8, pp. 608-616, August 2010.

[16] K. Suzuki, H. Kubota, S. Kawanishi, M. Tanaka and M. Fujita, "Optical Properties of Low Loss Polarization Maintaining Photonic Crystal Fibre," Optics Express, vol. 9, no. 13, pp. 676-680, 2001.

[17] R. T. Bise and D. J. Trevor, "Sol-Gel Derived Micro-Structured Fiber: Fabrication and Characterization," Optical Society of America, Optical Fiber Communications (OFC), Washington, DC, 6-11 March Conference, 2005.

[18] L. Xiao, W. Jin, and M.S. Demokan, "Fusion splicing small core photonic crystal fibers and single-mode fibers by repeated arc discharges," Optics Letters, vol. 32, no. 2, pp. 115–117, 2007.

[19] S. G. L. Saval, T. A. Birks, N. Y. Joly, A. K. George, W. J. Wadsworth, G. Kakarantzas, and P. S. J. Russell, "Splice-free interfacing of photonic crystal fibers," Optics Letters, vol. 30, no. 13, pp. 1629-1631, July 2005.

[20] G. S. Wiederhecker, C. M. B. Cordeiro, F. Couny, F. Benabid, S. A. Maier, J. C. Knight, C. H. B. Cruz, and H. L. Fragnito, "Field enhancement within an optical fibre with a subwavelength air core," Nature Photonics, vol. 1, no. 2, pp. 115–118, 2007.

[21] Y. Ruan, H. Ebendorff-Heidepriem, V. Afshar, and T. M. Monro, "Light confinement within nanoholes in nanostructured optical fibers," Optics Express, vol. 18, no. 25, pp. 26018–26026, Dec. 2010.